Identifying biosignatures on Planetary Surfaces with Laser-based Mass Spectrometry

Peter Wurz
Physics Institute, University of Bern, Sidlerstrasse 5, 3012 Bern, Switzerland
peter.wurz@unibe.ch

Marek Tulej
Physics Institute, University of Bern, Sidlerstrasse 5, 3012 Bern, Switzerland
marek.tulej@unibe.ch

Rustam Lukmanov
Physics Institute, University of Bern, Sidlerstrasse 5, 3012 Bern, Switzerland
rustam.lukmanov@unibe.ch

Valentine Grimaudo
Physics Institute, University of Bern, Sidlerstrasse 5, 3012 Bern, Switzerland
valentine.grimaudo@unibe.ch

Salome Gruchola
Physics Institute, University of Bern, Sidlerstrasse 5, 3012 Bern, Switzerland
salome.gruchola@unibe.ch

Kristina Kipfer
Physics Institute, University of Bern, Sidlerstrasse 5, 3012 Bern, Switzerland
kristina.kipfer@unibe.ch

Coenraad de Koning
Physics Institute, University of Bern, Sidlerstrasse 5, 3012 Bern, Switzerland
coenraad.dekoning @unibe.ch

Nikita Boeren
Physics Institute, University of Bern, Sidlerstrasse 5, 3012 Bern, Switzerland
nikita.boeren@unibe.ch

Loraine Schwander
Physics Institute, University of Bern, Sidlerstrasse 5, 3012 Bern, Switzerland
Loraine.schwander@unibe.ch

Peter Keresztes Schmidt
Physics Institute, University of Bern, Sidlerstrasse 5, 3012 Bern, Switzerland
peter.keresztes@unibe.ch

Niels F. W. Ligterink
Physics Institute, University of Bern, Sidlerstrasse 5, 3012 Bern, Switzerland
niels.ligterink@unibe.ch

Andreas Riedo
Physics Institute, University of Bern, Sidlerstrasse 5, 3012 Bern, Switzerland
andreas.riedo@unibe.ch

2022 IEEE Aerospace Conference (AERO) | 978-1-6654-3760-8/22/$31.00 ©2022 IEEE | DOI: 10.1109/AERO53065.2022.9843803

Abstract— **We present a Laser-based Mass Spectrometer (LIMS) for the sensitive, chemical (elements, isotopes, and molecules) analysis of matter as an analytical instrument on a landed spacecraft on planetary surfaces for the identification of signatures of life, extinct or extant. Our LIMS system is compact, features simple and robust operation, and is optimized for the detection of signatures of life, among others. The LIMS instrument can be part of the science payload on a rover or be part of an instrument suite on a landed spacecraft supplied by a common sample delivery system.**

The LIMS instrument is a reflectron-type time-of-flight mass spectrometer coupled to a pulsed laser system for the removal of material from solid samples for mass spectrometric analysis. Operating LIMS with high laser irradiances results in material ablation from the surface, which is used for element and isotope analysis. Moreover, when staying at the same spot the sequence of mass spectra resulting from these laser pulses can be used to derive a depth profile of the atomic composition at the sampled location, all the way to 3D composition analysis with high spatial resolution. Fossils embedded in a mineral host, as an example, can then be identified by their unique chemical signature compared to the host mineral(s), allowing us to study even single microbes. In addition, the measurement of isotope abundances, e.g. sulfur, provides additional information on biogenicity, the environment, and the metabolism of the life forms.

Alternatively, operating LIMS with low laser irradiances results in gentle desorption of chemical compounds, which is used for the detection of molecules and biomolecules present on the investigated surface. We obtain chemical information of molecules present on a surface, with a sensitivity down to fmol / mm^2, registering signals from intact complex molecules as well as their unique and simple fragment distribution, allowing for unambiguous chemical identification of the species. This allows for the study of biologically relevant complex molecules extracted from a surface sample, e.g. amino acids, lipids, polycyclic aromatic hydrocarbon, and other biomolecules with high sensitivity.

TABLE OF CONTENTS

1. INTRODUCTION

The detection of signatures of life, past or present, on planetary objects other than the Earth (e.g. Mars, Europa, Enceladus, or in the clouds of Venus) is of the highest interest in current space science. These signatures are of morpho-

logical and chemical nature, thus, requiring a specific set of instruments to detect them. For Solar System objects *in situ* detection of chemical and morphological signatures of life on planetary surfaces in extraterrestrial material is part of the following missions: NASA's Perseverance rover, which landed on Mars in February 2021, and the ExoMars astro-biology mission of ESA and Roscosmos, which is expected to land in April of 2023. The Perseverance rover landed in the Jezero Crater, in a dry lakebed, to look for signs of ancient microbial life. Imagery recorded by Perseverance of surface features near the landing site are indicative of ancient water flows and a persistent lake environment [1]. Perseverance will be able to drill, collect, and leave the packaged rock samples on the surface, which will be collected and returned to Earth aboard a future mission to be examined for potential biosignatures in terrestrial laboratories. The ExoMars rover has the scientific instrumentation to search for the existence of past and present life on Mars. Oxia Planum was selected as its landing site, which contains one of the largest exposures of rocks on Mars that are around 3.9 billion years old and contains clay-rich formations, indicating water processing and the presence of clement conditions. There is also a number of proposed future missions dedicated to the search of signs of life. Possible such missions are, for example, the Europa Lander of NASA [2], a mission to Enceladus [3], or search for life in Venus' clouds [4].

The most challenging technical application in chemical analysis of rocks found on Mars is searching for signatures of life. The SAM (Sample Analysis at Mars, an instrument based on classical gas-chromatograph mass spectrometry [5]) measurements on the Mars Curiosity rover show that organic matter is preserved in lacustrine mudstones at the base of the ~3.5-billion-year-old Murray formation at Pahrump Hills, Gale crater [6]. However, the observations do not determine the source of the organic matter, biological, geological, and meteoritic sources are all possible. On the ExoMars rover of ESA, to be launched in 2022, this goal will be pursued with the MOMA instrument [7, 8], the most recent implementation of a mass spectrometric experiment with gas-chromato-graphy and laser desorption front-ends.

Searches for signs of extinct or extant life on a planetary body require sensitive techniques and novel analytical approaches capable of delivering high-quality chemical information at the spatial scales of the expected life form. In particular for the preparation of the ExoMars mission the conclusiveness of various chemical signatures for the detection life has been studied in great detail [9, 10]. Considering that life forms on the Martian surface likely will be sparsely distributed within the analyzed sediments (sparse life), this means one must search for individual microbes, or perhaps small colonies (fossils or alive), which requires spatial resolution at the few µm scale [11, 12].

Chemical analysis on the surfaces of planetary bodies is a challenging endeavor, imposing a set of specific parameters the onboard instrumentation must comply with. This applies to the quality of information gathered from a wide range of samples, the size and power consumption of the instrument, the ability to operate mostly autonomously, and to survive the harsh environmental conditions. Therefore, only a small subset of analytical methods known from the laboratory qualifies as space applicable. Here, we summarize potential biosignatures that can be detected and characterized *in situ* on a planetary surface with our integrated LIMS system (mass spectrometer combined with a laser ion source and a microscope).

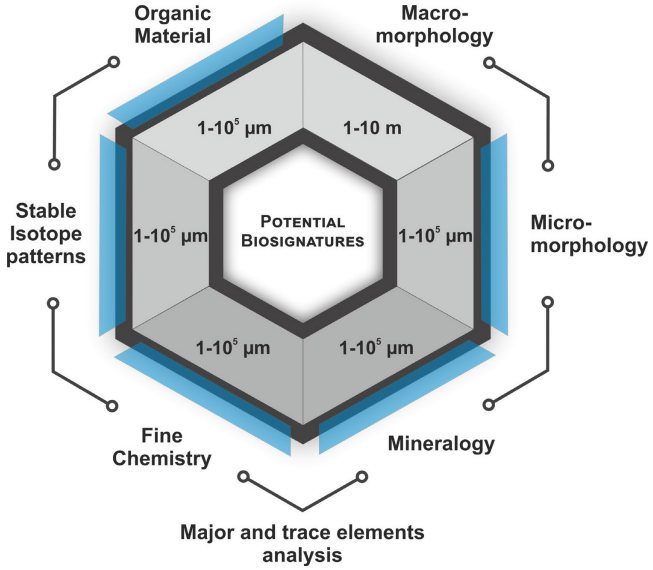

Figure 1: The six major groups of potential biosignatures, and the range of their spatial extent in a sample, as proposed by the Mars 2020 science definition team [13]. Applicability of the LIMS (ablation and desorption mode) combined with its microscopy system in the identification of potential biosignatures is indicated by the blue sections.

There is a wide range of biosignatures that applies to the LIMS technology for its identification from macroscopic scales down to the scale of individual microbes. Figure 1 summarizes the different types of potential biosignatures and the range of their spatial extent. The subset of these biosignatures that can be addressed by the LIMS technology are indicated, which are the micromorphology (via the microscopic camera systems), the molecular composition of organic matter, and fine chemistry of element abundances, and the isotope abundances (all via the LIMS instrument). Furthermore, the mineralogy on a microscopic scale can derived from the measured element abundances.

In the following we will give examples for these diverse measurements for the detection of biosignatures using our LIMS instrument. Naturally, detection of a single biomarker shown in Figure 1 is not enough to claim the detection of life. Detection of a combination of several of them, perhaps supported by the detection of additional ones by different instruments, if available, will make it possible to identify the presence of life at the microbial level [13].

The value of an analytical technique for the identification of a biosignature can be scored on the generalized hexagon of potential biosignatures, as proposed by the Mars 2020 science

definition team [13], see Figure 1. The binary scoring board presents six groups of potential biosignatures and identifies the value of applied methods. Broadly, the hexagon scheme can be divided into two big sections which are morphological biosignatures and chemical biosignatures. Morphological biosignatures deal with different types of imagers that are required for the identification of: 1) macroscopic-scale structures (such as stromatolites), and 2) imaging of microscopic-scale structures (i.e., individual microfossils and bio-lamination sites). Although the first group is primarily addressed by cameras working in the visible range, it also includes methods like ground penetration radar and hyperspectral imaging.

The second large group of potential biosignatures uses the detailed characterization of the chemistry of samples. Naturally, the first subgroup of the chemical biosignatures addresses the determination of mineralogical compositions. Considering the overall diversity of minerals, this subgroup places hard requirements on analytical methods, meaning that the ideal method should apply to a wide range of minerals. The second subgroup of chemical biosignatures requires the determination of fine chemistries, i.e., rare earth element concentrations, which are also very challenging to measure for most analytical methods because of their low abundance that typically lie at the ppm abundance level. The third subgroup refers to measuring the isotope fractionation resulting from biological metabolism of elements. Isotope fractionation on the microscale level, if measured correctly, can strongly indicate biological processing. However, among the available groups of potential biosignatures, identification of the isotope abundances on the microscale places the harshest requirement on measurements, because of the required accuracies. And lastly, the fourth subgroup of chemical biosignatures presents the importance of molecular characterization of investigated materials.

2. The LIMS Instrument

Laser ionization mass spectrometric (LIMS) measurements were conducted using our prototype mass spectrometer instrument built at the University of Bern. The system was originally designed for the *in situ* chemical analysis of solids (for elements and isotopes) on the surface of planetary bodies [14]. For more than two decades, we designed, developed, and operated a fully functional flight-size LIMS prototype instrument for in situ research on planetary surfaces in our laboratory. Detailed information about the design and the details of operation can be found in previous publications [see e.g., 15, 16, 17, 18, 19, 11, 20, 21, 22]. In the following only a brief description of measurement principles is given.

The schematics of the current measurement set-up and LIMS principles of operation are illustrated in Figure 2. The LIMS system consists of a miniature reflectron-type time-of-flight mass spectrometer (RTOF, analyzer with geometrical dimensions of 160 mm x Ø 60 mm, installed within vacuum chamber with typical base pressure of mid 10^{-8} mbar), which is coupled to a pulsed laser system for removal and ionization of sample material. The laser beam is guided through the center of the mass analyzer towards the sample surface and focused to small spot sizes, with the sample being placed just at the entrance of the ion optical system (see Figure 2). The positive ions created by the laser pulse hitting the surface are

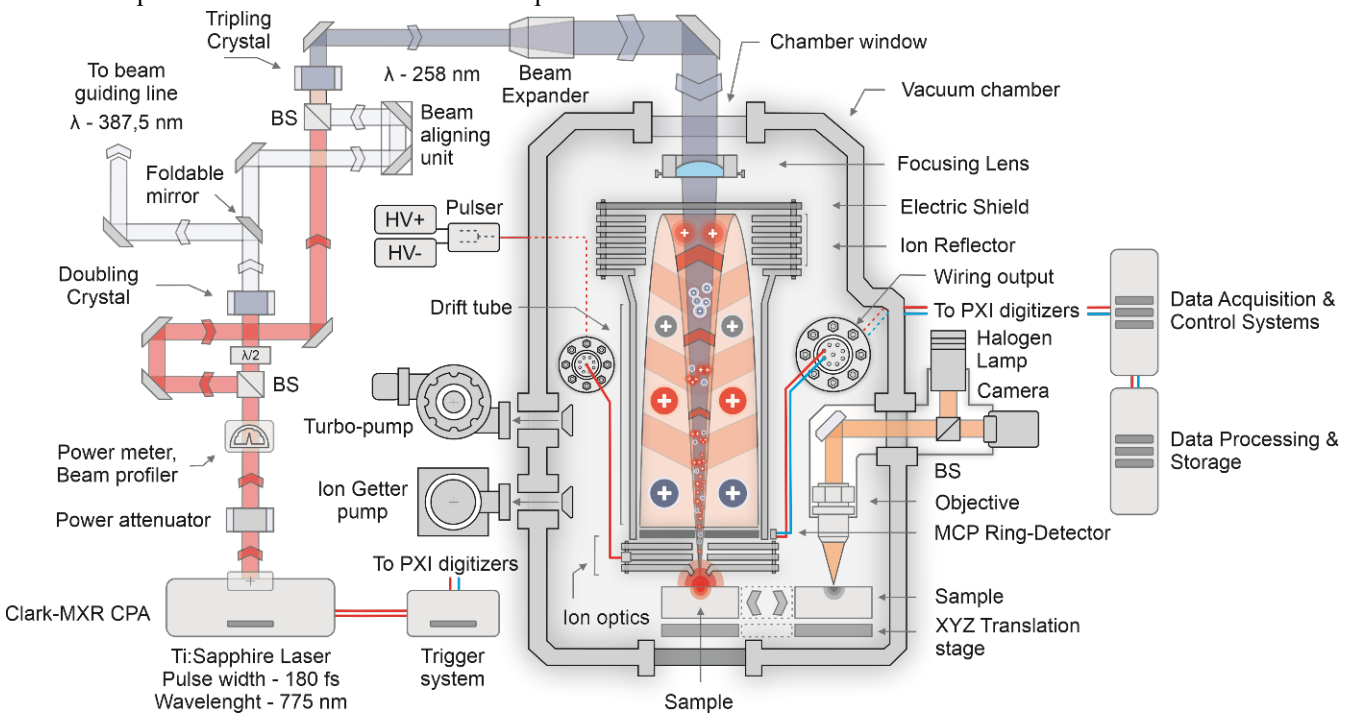

Figure 2: Schematics of the laser beam guiding and subsequent mass spectrometric analysis of ablated positive ions with LIMS. The displayed laser system provides three wavelengths (775 nm, 387 nm, and 258 nm) to be used for ablation. See text for more details.

accelerated into the TOF section for mass analysis. The ions directly enter the mass analyzer, and are accelerated, confined, and focused to the field-free drift path. At the ion mirror (reflectron), the ions are reflected towards the detector system by passing the drift path a second time. TOF spectra are recorded with a high-speed measurement system (8-bit vertical dynamics, up to 4 GS/s), and an in-house written software-suite was used for the data analysis that includes e.g., signal integration, conversion of TOF to mass spectrum [23]. The sample holder is positioned below the mass analyzer on a three-dimensional translation stage with micrometer position accuracy. A high-resolution microscope camera system is installed to the mass analyzer to allow accurate targeting of surface material. The camera system has a spatial resolving power of 1 µm [24].

The present performance of our LIMS system provides a mass resolution m/Δm of up to about 1100, a wide mass range of 1 – 1000 u, an accuracy of the mass scale of 500 ppm, and a dynamic range of 8 decades. LIMS measurements provide full mass spectrometric analysis, enabling detection of trace elements at the ppm level down to 10 ppb depending on mass, desorption of biomolecules at surface concentrations down to fmol mm^{-2}, and isotope measurements with accuracies at the per mile level for biologically relevant isotope systems, all within seconds.

In laser ablation mode we use a femtosecond laser system (fundamental wavelength λ = 775 nm, or the harmonics at 378 nm and 252 nm, laser pulse repetition rate of 1 kHz) and high laser irradiances of the order of TW/cm^2 (corresponding to a few 10^{-1} J/cm^2). The laser beam is focused through the mass analyzer to spot sizes of about 8 µm in diameter onto the sample surface. With every laser pulse about 10 femtograms of sample material are removed, with spatial dimensions of about 5–10 µm in lateral direction, given by the laser spot diameter on the sample, and an ablation depth in the nanometer range. Since we operate not far above the threshold for material ablation, we obtain almost complete atomization of the removed material, and homogeneous ionization. The laser ablation mode is used for quantitative element and isotope analysis of almost all elements. The formation of small particles of 10 – 1000 nm during laser ablation, as it is commonly observed in LA-ICP-MS [25], is not observed here. Note that ablation in LA-ICP-MS instruments operates at higher laser intensities of 10–60 TW/cm^2 (corresponding to several J/cm^2) and operates in a gas atmosphere.

To increase the sensitivity and improve quantitative measurements, the laser ion source can be operated in double laser pulse mode where the initial laser pulse is divided into two pulses with equal energy, with one laser pulse delayed with respect to the other. The double pulse mode optimizes the ion production by post ionization of neutrals ablated by the first laser pulse. For single pulse operation, the ionized fraction in the plume of ablated material is about 0.1%, for double pulse operation the ion fraction can be increased to up to 10%. The pulse delay for efficient post-ionization of the generated ablation plume was found to be in the range of 20 – 30 ps. Further details about this double pulse ion source can be found in our previous publications [26, 27].

Operating LIMS in desorption mode, with low laser intensities of the order of few 100 MW/cm^2 results in gentle desorption of chemical compounds, which is used for the detection of molecules and biomolecules present on the investigated surface. Here we use a nanosecond pulsed Q-switched Nd:YAG laser (λ = 266 nm, pulse duration ~ 3 ns, pulse repetition rate of 20 Hz) providing a focal spot size of 30 µm. Low laser irradiances on the sample cause the desorption of neutral and ionized atoms and even intact molecules from the sample surface [28]. LIMS operation in desorption mode has previously been described in detail in [29]. The coupling of the laser to the mass spectrometer for LIMS in desorption mode is similar, but slightly simpler, compared to the operation in ablation mode. Again, the sample is placed just at the entrance of the ion optical system. Molecular and biomolecular samples are prepared in solutions that are drop-casted into small cavities of the sample holder [30]. After evaporation of the solvent, the samples are introduced into the vacuum system for analysis with the LIMS instrument.

3. Element Composition Analysis

Our LIMS instrument is built for the quantitative measurement of element abundances in the sample, which has been discussed in previous publications in detail [16, 14, 20, 30, 31, 32]. Typically, the quantification of element abundances by our LIMS is comparable to laboratory LA-ICP-MS instruments with uncertainties for the abundance quantification of about 10%, which is reviewed in [14]. Measuring the element composition of a sample from a planetary surface allows us to distinguish between the host material (the inorganic matrix) and the life matter (e.g., biomolecules, bio-organic remains, or microbes themselves). This is true for fossils and even more so for present life. The rough chemical composition of simple life (dry bacteria) is: H 48.7%, O 16.7%, C

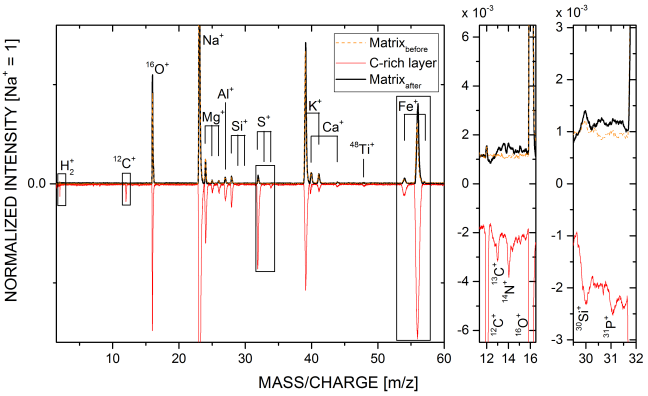

Figure 3: Identification of single-cell microbial life using LIMS [12]. Mass spectra pointing upwards: chemical information of sample material just above and below the microbe. Note that both traces (solid black and dashed orange) agree very well with each other. In red the chemical pattern of the microbe is shown. In comparison to the host material, elements such as C, H, N and P show an increased abundance.

29.9%, and N 4.7% given in atomic fractions [34]. In addition, there are minor amounts of Ca, P, K, Na, Cl, Mg and S present as well. The elements C, H, N, O, P, and S (represented by the acronym CHNOPS) are the six key chemical elements in biological molecules on Earth and are expected for aqueous-based life elsewhere. As a first step in the search for signs of life, looking e.g., for significant increases in carbon will give a potential location of microbes in a sample, since C is low in the typical host minerals like clay. Once a carbon-rich location is found, the sample location is investigated for the presence of other biologically relevant elements, to conclusively indicate the presence of microbes.

In an earlier study Mars analogue mudstone materials were investigated [11], where the samples were analyzed with LIMS in ablation mode to measure the element composition along a depth profile in nanometer steps per laser shot. Half of these samples were artificially inoculated with microbes with a density of about 10^6 cells/cm^3, which is only slightly higher than the cell density in the most arid places in the Atacama Desert [35, 36], which is a well-known analog field site for Mars research. Starting with the search for intense carbon signals (a strong indicator for life, as described above), regions in the sample that showed a high abundance in carbon could be identified. Such locations were identified in both sets of samples, those with and those without microbes. However, as shown in Figure 3, only in life-containing samples the other important elements for life, such as H, N, P, O, and S could be identified together with the carbon [12]. Moreover, the number of such positive detections by LIMS matched the cell density of inoculated microbes, thus the detection efficiency for single microbes is about 100%. This measurement represents the first demonstration of the detection of single-cell microbes using a potential instrument for *in situ* planetary research. Also, the abundance of these elements matched the expected atomic composition of life, including the lower abundance of O in the microbe compared to its abundance in the host mudstone material.

The study with the Mars analogue mudstone materials also demonstrated that sparse life in a sample will only be detected with instrumentation probing at the appropriate spatial scales of the microbes [11,12]. Established laboratory instrumentation probing at larger spatial scales, i.e., performing bulk analysis failed to detect these microbes dispersed in the sample [12].

Considering sparse life and a heterogeneous distribution of microbes in a soil sample, as expected for Mars, the 1D analysis (i.e., the depth profile) might not be enough to locate microbes in sufficient quantities. With LIMS, one can analyze complete volumes by rastering the laser beam over a sample. Each laser shot produces a mass spectrum, and these spectra can be processed to obtain the 3D distribution of elements in the investigated volume of the sample [37, 38].

Figure 5 shows the heterogeneous distribution of S impurities from a 3D composition analysis of a SnAg alloy as an example [37]. The average abundance of the S impurity over the investigated volume (i.e., the bulk abundance) in this

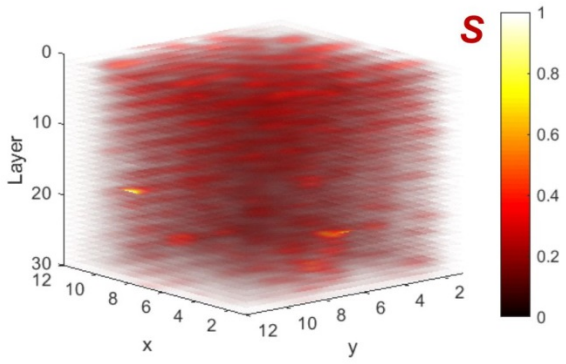

Figure 5: 3D composition analysis of a SnAg alloy showing the heterogeneous distribution of S impurities [38]. The displayed volume is 20 µm in the *x* and *y* directions, and the vertical depth is about 2 µm.

sample is about 0.5%. The S impurity in this sample displays a very heterogeneous distribution, visible as local variations in S abundance spanning orders of magnitude on spatial scales of µm. Similar results are expected for the search of sparse life in Martian soil samples. Assuming 10^3 cells/mm^3 for sparse life, one would expect to detect about 1 microbe in the sampled volume of $V = 10^{-3}$ mm^3. However, one can go much deeper with the 3D analysis by the laser [38], up to about 50 µm, which would then give about 25 detected microbes.

4. Multi-dimensional Element Analysis

Moving the laser spot over the sample allows for chemical maps of the surface, i.e., 2D chemical analysis, and doing that repeatedly even allows for 3D chemical analysis of a sample [14], as shown in Figure 5, which allows studying chemically heterogeneous samples at micrometer lateral scales and nanometer depth scales. 2D or 3D analysis can be used to identify and analyze microscopic fossils on the surface [39] or in the bulk [33].

Figure 4 shows optical microscopy images of the analyzed area on the Gunflint sample, with entrapped fossils of microbial life that existed almost 2 billion years ago [39, 40]. Areas with a high density of microfossils appear dark in these images, lighter areas are mostly the host mineral, the chert. About six genera of microbial life can be identified in this sample.

The chemical maps of the bio-relevant elements C, H, N, O, P, and S recorded with LIMS in ablation mode are shown in

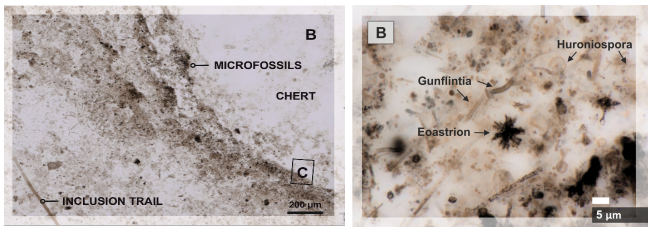

Figure 4: Left: Optical microscope image of the analyzed area on the Gunflint sample. Right: Detail showing some microbial fossils entrapped in the sample.

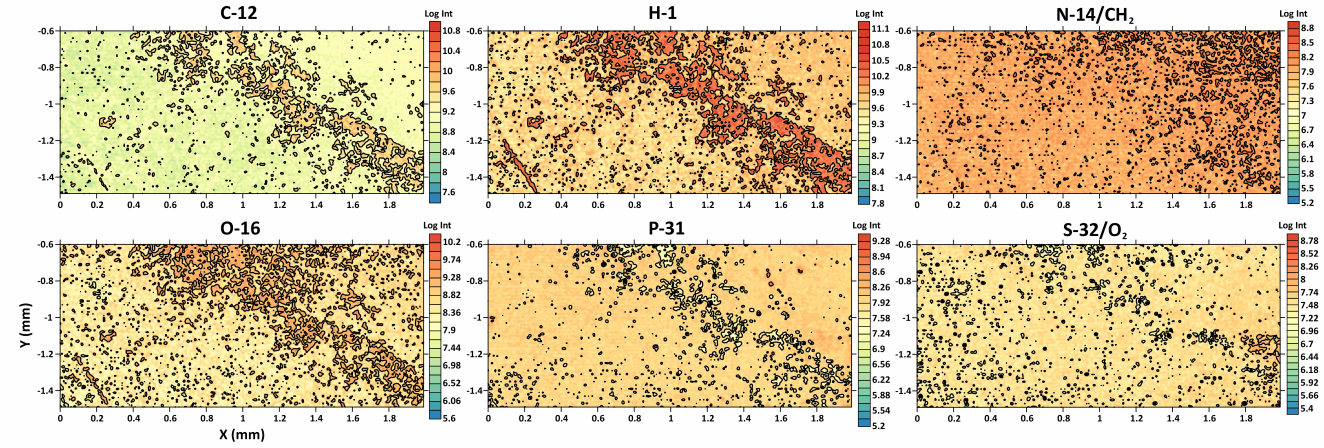

Figure 6: Intensity maps of the Gunflint sample. The chemical maps of C, H, N, O, P, and S are shown. The bio-lamination surface with organic material in the upper right corner can be seen in maps of C, H, and O.

Figure 6 in the six panels of element maps. These bio-relevant elements clearly trace the areas of the microbial fossils, when compared to the microscope image of the sample shown in Figure 4. The bio-lamination surface from the aggregation of microfossils can be identified in ^{12}C, ^{1}H, and ^{16}O maps appearing in the upper right corner of the images, as is discussed below. The low-intensity regions in the element maps correspond to the quartz matrix.

Having mass spectra from a 2D or 3D array of locations on the sample makes for a large dataset with a quite complex internal structure. Such large and complex datasets produced by LIMS can be further analyzed using dimensionality reduction and manifold learning techniques to detect signatures of different chemical entities in the sample, e.g. the different minerals and microfossils [40, 41]. Using principal component analysis (PCA), the LIMS dataset was reduced down to the first 60 principal components by removing the empty dimensions dominated by noise from the original dataset. The Uniform Manifold Approximation and Projection (UMAP) algorithm [42] was used to further characterize non-linear dependencies present in the PCA reduced data matrix. The overall classification of the UMAP scores was made using a hierarchical density-based clustering algorithm (HDBSCAN). Figure 7, left panel, shows the low dimensional structure of the imaging data cube (originally 260-dimensional data) of the Gunflint sample revealed by UMAP. The point cloud data are plotted along with the isodensity surface. The point cloud data are plotted along with the density surface. The low-triangulated mesh represents the volumetric isodensity surface of UMAP scores calculated from the 18'000 LIMS mass spectra from the 2D set of locations. Three entities are identified based on the spectral neighborhood: the host mineral (quartz), the microfossils, and the surface contamination.

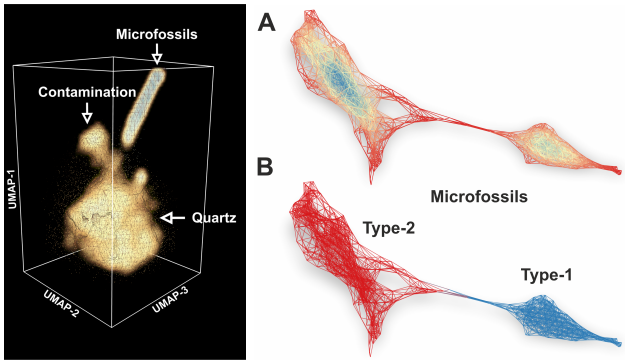

Figure 7: Left: Low dimensional structure of the imaging data cube revealed by UMAP [40]. Triangulated mesh represents volumetric isodensity surface of UMAP scores calculated from the 18'000 fs-LIMS mass spectra. Right: Spectral similarity network constructed from 1'964 LIMS mass spectra registered from the microfossils [40]. Each node represents a single or a group of spectra with a significant similarity of intensity profiles. The edges connected with nodes indicate that nodes have one or more shared spectra. The network is colored according to the eigenvector centrality of nodes.

The subset of mass spectra identified from the microfossils were further visualized using the Mapper algorithm [43, 41] (see Figure 7 right panel), where identification of the entities present in this subset was conducted using a greedy modularity optimization algorithm, i.e., the Louvain modularity. Figure 7, right panel, shows the spectral similarity network constructed from 1'964 LIMS mass spectra registered from the microfossils, where each node represents a single or a group of mass spectra with a significant similarity of intensity profiles. The edges connected with nodes indicate that nodes have one or more shared mass spectra. The network on the top (Figure 7, right panel) is colored according to the eigenvector centrality of nodes and indicates a presence of variability of spectral profiles within a specific group (blue nodes indicate more central nodes in the network, and red nodes indicate fewer central nodes). The first three UMAP components were used as a lens (mapping space) to project the data into a single network using the Mapper algorithm. The proximity of nodes in the network identifies two groups of microfossils and a transition structure between two classes. Panel B (Figure 7, right panel) shows the Louvain clustering of the spectral similarity network. The blue part of the network identifies type-1 microfossils, and the red part of the network illustrates spectra registered from the type-2 microfossils.

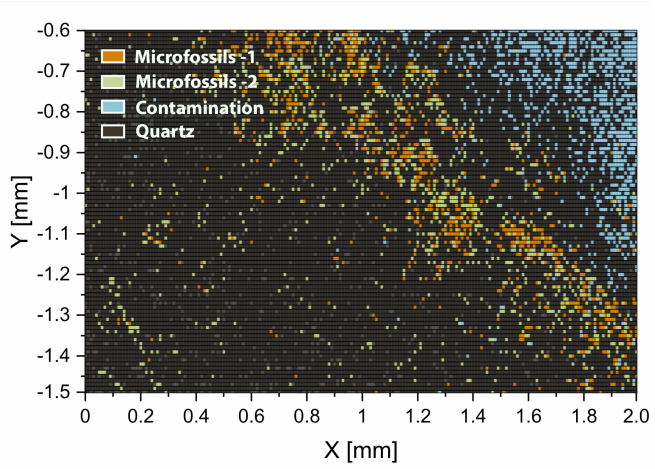

Figure 8: Different entities identified in the Gunflint sample [40]. The orange pixels represent spectra registered from the type-1 microfossils, green pixels represent spectra registered from the type-2 microfossils, the blue pixels represent spectra registered from the surface contamination. Black and grey pixels are spectra registered from the quartz matrix of the Gunflint chert. Compare to the optical microscopy image of the analyzed area shown in Figure 4. Note the aligned distribution of classified spectra with the bio-lamination surface crossing the image.

With the method described above we have identified the different entities present in the sample, i.e., the host mineral (quartz), the two types of microfossils, and a modern organic contamination on the surface. Since each mass spectrum is associated with an entity, a map of the spatial distribution of these entities can be drawn since localization of the mass spectra on the sample surface is know from their recording. Figure 8 shows the spatial distribution of the identified entities from the hierarchical density-based spatial clustering (HDBSCAN) of six UMAP components of the LIMS dataset. Note the geometric agreement of the distribution of classified spectra with the bio-lamination surface crossing the image shown in Figure 4, left panel.

5. Isotopes as Bio-Signatures

Ratios of stable isotopes of elements that participate in the metabolic cycle of lifeforms are often used as biosignature, for example $^{13}C/^{12}C$, $^{15}N/^{14}N$, $^{34}S/^{32}S$, and $^{56}Fe/^{54}Fe$. Element isotope fractionation signatures are very robust against degradation by the harsh environmental conditions, such as temperature or irradiation, which typically prevail on and near the surfaces of Solar System bodies. However, the measurement of isotope ratios *in situ* on a planetary surface is extremely challenging because of the high accuracy that is usually required.

We determined the accuracy of isotope abundance measurements of our LIMS instrument as function of the abundance of species using NIST steel reference samples [44, 43, 14]. Because of decreasing signal-to-noise the accuracy degrades with lower isotope abundance, but the accuracy still is sufficient for in situ planetary research for species at the 10 ppm level. We will show two examples of isotope measurements in the following.

Sulfur is a key element for life as we know it and there are known types of bacteria, such as sulfur reducing bacteria, that can metabolize sulfur with resulting isotope fractionations of up to $\delta^{34}S = -70‰$. Geochemical processes are observed to fractionate up to values of $\delta^{34}S = 20‰$, meaning fractionation exceeding that value might be highly indicative for the presence of life.

To investigate the possibility of using $^{34}S/^{32}S$ isotope ratios as a biomarker, we studied five representative terrestrial samples from three different field sites using our LIMS instrument [46]. Three samples originate from the river Río Tinto (named RT1, RT2, RT6), Spain [47], one sample is collected from the Movile Cave (named MC) [48, 49, 50], and one sample is obtained from the Sulfur Cave (named SC) [51], which are both located in Romania. These three field sites were selected for sulfur samples because they reflect some environmental conditions that prevailed, or may still be prevailing, on Mars. The samples selected for this study cover a wide range in their sulfur content, with weight fractions from 5.7% for RT1, 14.9% for RT3, 15% for MC, 30.2% for RT2, and 96.5% for SC. Reference measurements for the isotope fractionation and sulfur content were performed externally with state-of-the-art isotope mass spectrometry [46].

Figure 9 shows our LIMS measurements in ablation mode together with the reference values from the laboratory instrument. The LIMS measurements, the sulfur abundance and the $^{34}S/^{32}S$ isotope ratios, agree well with the reference values measured with state-of-the-art sulfur isotope analysis technique. The errors of the reference measurements are very small, smaller than the symbol size used in Figure 9. The

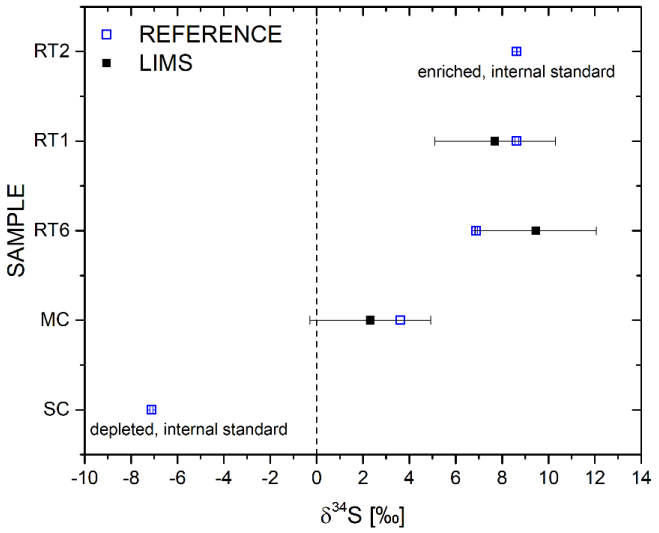

Figure 9: Comparison between measured values and reference values for $\delta^{34}S$. Three samples are from the river Río Tinto, Spain (RT1, RT2, RT6), one sample is from the Movile Cave, Romania (MC), and one sample is from the Sulfur Cave, Romania (SC).

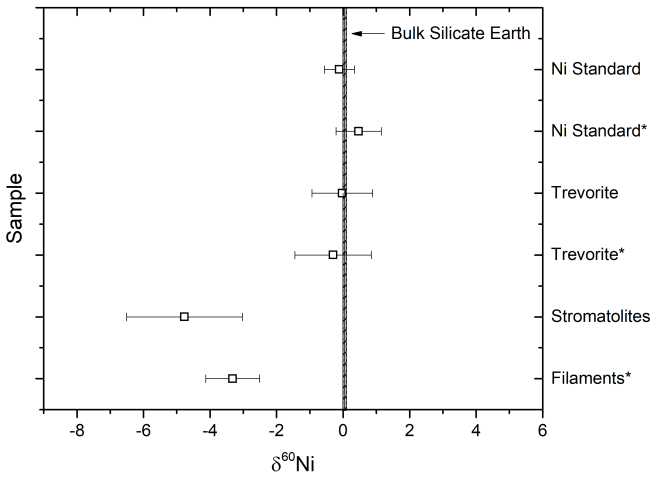

Figure 10: Comparison of δ^{60}Ni isotope values from LIMS measurements of this study. δ^{60}Ni isotope values for Ni standard NIST SRM 986, Trevorite, Stromatolites, and Filaments are shown [54]. The * refers to values of an earlier study using the same LIMS instrument. The vertical line refers to Bulk Silicate Earth [52].

obtained measurement accuracy of our LIMS instrument for the sulfur isotopes is sufficiently high to provide valuable information on geochemical processes or to indicate life in case of the presence of e.g., sulfate-reducing bacteria, which may fractionate sulfur isotopes clearly above $\delta^{34}S = –20‰$. For our LIMS measurements we estimated an error of $\delta^{34}S \sim 2‰$, and our results agree with the reference measurements within this error. In addition to the sulfur isotopes, the LIMS measurements simultaneously provide detailed element composition information to study the context of mineralogy and characterize the microbial community.

An interesting, yet challenging, goal for an isotope study was the investigation of the $^{60}Ni/^{58}Ni$ isotope abundances from microscopic structures, possibly fossils of methanogens, in samples that were collected from the slow-spreading Mid-Atlantic Ridge at a depth of 27 m below the seafloor during the Ocean Drilling Program Leg 209 [53]. Methanogenesis (and, concomitantly, methanogens) thrived in the chemo-synthetic dominated biosphere before the great oxidation event, which occurred approximately 2.4–2.0 billion years ago. An unique Ni co-factor is at the active site of essential enzymes in multiple strains of methanogens. Fractionation of Ni isotopes towards the enrichment of the lighter isotopes has been shown for several studied methanogens and is assumed to have occurred in these ancient methanogens as well. Since the methanogens require Ni for their survival, the composition of Ni isotopes in the sample can be indicative of fossils of that time, and perhaps of similar fossils on Mars.

Figure 10 shows several LIMS measurements in ablation mode of the $^{60}Ni/^{58}Ni$ isotope ratio, from the Ni standard NIST SRM 986, the Trevorite mineral (a mineral standard), and for the microfossils of the sample [54]. The Trevorite mineral, a rare nickel-iron oxide mineral belonging to the spinel group, serves as a reference sample.

Comparisons of the δ^{60}Ni isotope measurements with the Ni standard NIST SRM 986 and the Trevorite mineral show sufficient accuracy in the Ni isotope measurement of about 1 per mil using our LIMS instrument (see Figure 10). Because of the high spatial resolution of our LIMS system, we can investigate the microscopic fossils of stromatolite and filament embedded in the aragonite veins individually. We find that the δ^{60}Ni isotope values show that light isotopes are enriched in these fossilized microorganisms in basalts (see Figure 10). In addition, we measured abundances of many trace elements such as O, Mg, Si, Mn, Co, S, C, Fe, and Ni providing the mineralogical context and environmental background of the embedded fossils [55].

6. Chemical Bio-Signatures

If life ever existed on a planetary body organic remains will have been left in its environment. As chemical bio-signatures, one looks for some of the most common molecules associated with terrestrial life. Amino acids and hydrocarbon derivatives associated with biogenic lipids have been argued by many to be present if life has formed elsewhere in the Solar System [48, 49]. Thus, the mass spectrometric detection and identification of a range of organic molecules, such as amino acids and lipids, would be a strong biosignature. In addition, Polycyclic Aromatic Hydrocarbons (PAHs) are of interest, because of their potential role in the emergence of life and their abundance in the interstellar medium. Although PAHs are not known to be synthesized directly by biological processes [58], they could be precursors of molecules important for life [59]. However, distinction from abiotic sources is important, since several compounds of these chemical classes have been detected in meteorites. For example, amino acids, nucleobases, carboxylic acids, polyols, and hydrocarbons have been detected in the Murchison meteorite [60, 61].

Amino acids are among the most widespread biomolecules on Earth. Life on Earth uses 22 amino acids, while over 70 amino acids have been detected in meteorites [62, 63]. More than 500 naturally occurring amino acids are known [64]. The amino acids used by life on Earth constitute monomer units of polypeptides, including proteins. The processes that govern the production of amino acids, and the resulting pattern in the distribution of those amino acids, differ markedly between biological and abiotic systems [65]. Abiotically produced amino acids have abundance distributions driven by thermodynamics and kinetics [66], which contrasts with biotic amino acid distributions that are driven by functionality.

Since abiotic processes can yield a diverse inventory of organic compounds as well, including many species that are utilized in the biochemistry of Earth's life, one has to measure the abundances of the different amino acids in the sample to decide between a biotic and an abiotic origin. With a mass range from 1 – 1000 u, LIMS can capture a wide range of molecular structures diagnostic of biotic or abiotic origin, either individually or in their broad distribution. These include amino acids, lipids (fatty acids, prenols), sugars, nucleobases, PAHs and related structures, and potential

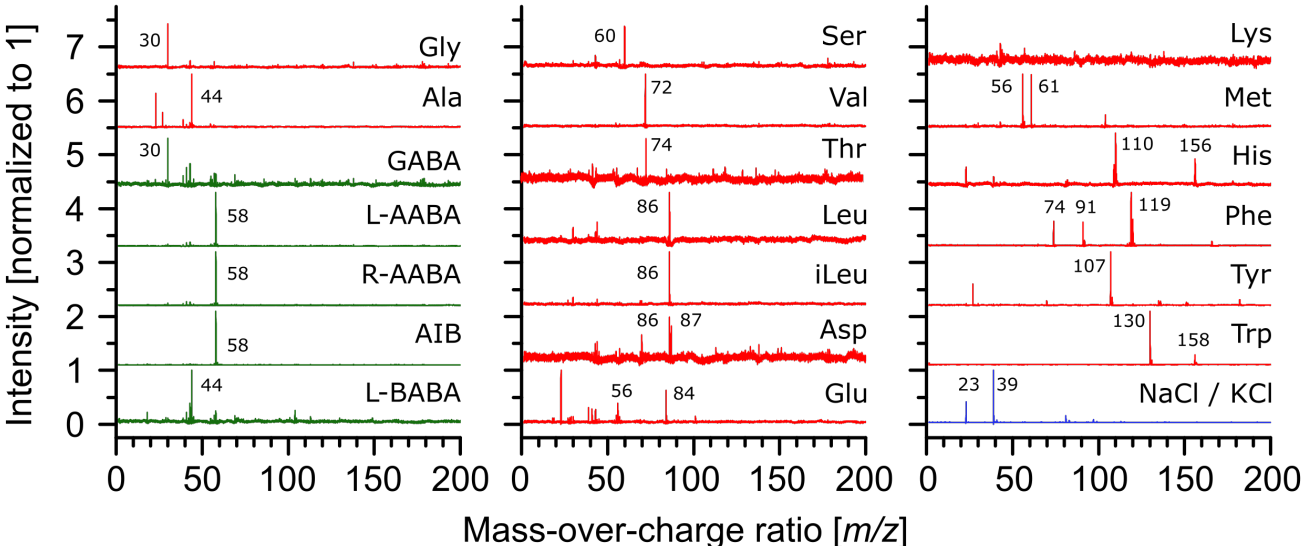

Figure 11: LIMS mass spectra in desorption mode of various biotic (red) and abiotic (green) amino acids, and of a mixture of NaCl / KCl salt (blue) [29]. Average surface concentration is 14 pmol mm^{-2} for the pure amino acids, and ~0.7 µg mm^{-2} for the mixture with NaCl / KCl salt. The primary fragments are labelled with their mass.

oligomers; as well as the myriad smaller catabolic products resulting from metabolic processes.

To investigate the potential of LIMS in desorption mode for the detection and identification of these molecular biosignatures, samples were produced by dissolving biomolecules in solutions at nM to µM levels, and drop-casting volumes of one to several µL of these solutions onto a sample holder. After the solvent evaporated and a film of organic material was formed, these samples were introduced into the LIMS system for measurements. In flight, these biomolecule extracts would be provided from a natural ice sample (e.g., Europa surface) or from a dedicated solvent extraction instrument. For example, by ExCALiBR [67], which performs solvent extraction of target lipids (fatty acids, alkanes, and polycyclic aromatic hydrocarbons) and purification from a regolith sample for molecular characterization by analytical instruments, like LIMS.

Figure 11 shows LIMS measurements in desorption mode of biotic and abiotic amino acids [29]. One requirement in the Europa Lander Science Definition report [65] is the detection of eight of the following amino acids: Ala, Asp, Glu, His, Leu, Ser, Val, Iva, Gly, β-Ala, GABA, and AIB[1]. We successfully measured ten of these amino acids with our LIMS instrument (β-Ala and Iva were not included in the study). The mass spectra of the amino acids are simple to interpret, they generally show high-mass fragment peaks of the side group or the amino acid stripped of its acid group, and in some cases the intact parent molecule peak. This unique pattern for each amino acid can be used to decompose the mass spectra and identify all amino acids and their relative abundance in a mix of amino acids.

Salts are a very likely contaminant in natural samples since they dissolve well in water, and water is the solvent for the amino acids, either because ice samples are collected (e.g. Europa lander) or from the extraction process. Fortunately, the presence of NaCl or KCl salts in the sample does not interfere with the detection of amino acids by LIMS.

With our LIMS setup operating in desorption mode we established the 3σ limits of detection ($LOD_{3\sigma}$) for amino acids, which are displayed in Figure 12. We measured amino acids down to a surface concentration between 1 and 600 fmol mm^{-2}, depending on the amino acid [29]. According to the Europa Lander Science Definition report [65], the Organic Composition Analyzer (OCA) needs to be able to detect

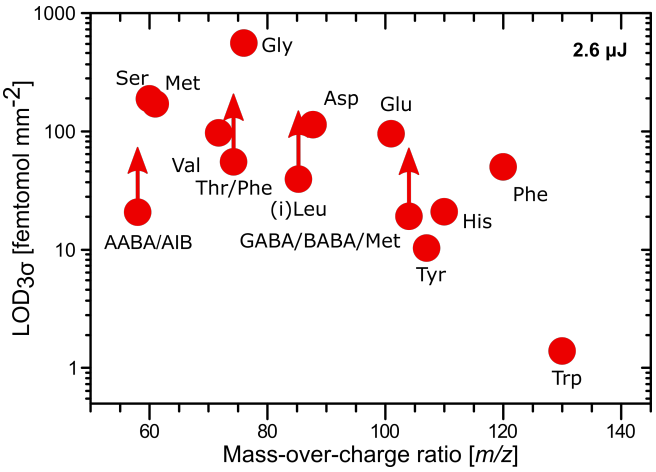

Figure 12: 3σ limits of detection ($LOD_{3\sigma}$) for amino acids calculated from the LIMS measurement at 2.6 µJ laser pulse energy [29]. Lower limits are given for signals that are detected but have contributions from multiple amino acids.

[1] The used abbreviations of amino acids are: Ala: alanine, Asp: aspartic acid, Glu: glutamic acid, His: histidine, Leu: leucine, Ser: serine, Val: valine, Iva: Isovaline, Gly: glycine, β-Ala: β-alanine, GABA: Gamma aminobutyric acid, and AIB: α-aminoisobutyric acid.

organic species at 1 pmol in a 1-gram surface sample (about 1 mL of water ice). Melting a 1-gram ice sample and producing an organic film on a surface area similar to the surface area of the sample cavities used in this work (7.1 mm^3) results in an average surface concentration of 146 fmol mm^{-2}, a surface concentration easily detectable by LIMS in desorption mode. With these LODs our LIMS system is more sensitive by 1–3 orders of magnitude, depending on amino acid, than the LDI linear ion trap instrument with a $LOD_{3\sigma} \leq$ 1 pmol mm^{-2} [7], which is part of the MOMA suite on the ExoMars rover.

All known living organisms possess lipid membranes, for compartmentalization, protection, and selective passage of molecules and ions. Thus, the presence of lipids is a strong biomarker for past and present life. Moreover, different domains of life (archaea, bacteria, eukarya) use different types of lipid membranes [10]. Fortunately, lipids and their fossil counterparts, i.e., hydrocarbon molecules, are very stable over geologic time scales [10]. Figure 13 shows two mass spectra of prenol lipids, with intensities normalized to the most intense peak, where 200 pmol vitamin K_1 (top) and α-tocopherol (bottom) were drop-casted for analysis. The most intense mass peak in the spectra was identified as the parent peak for both vitamin K_1 and α-tocopherol (see labels). The molecular structures of both lipids are shown in their corresponding mass spectra. The grey boxes in both mass spectra denote the contribution of sample holder contamination. Several other lipids were successfully detected with our LIMS instrument in desorption mode [68], which were menadione (vitamin K3), retinol (vitamin A1), cholecalciferol (vitamin D3), and ethynylestradiol.

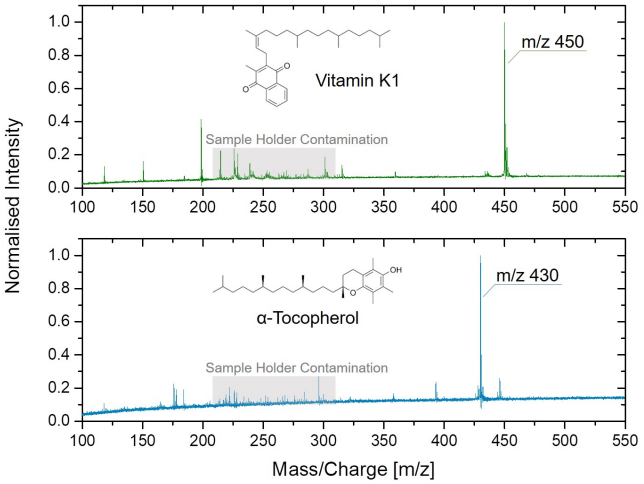

Figure 13: Mass spectra of two lipids recorded using our LIMS system operated in desorption mode [68]. The top panel shows Phylloquinone (vitamin K1) and the bottom panel shows A-tocopherol (vitamin E).

PAHs are compounds consisting of multiple aromatic rings and thus are stable chemical structures. In particular large cata-condensed PAHs (with decreased H/C ratio) are particularly stable to chemical modification. Aromatic units would therefore be robust against destruction by temperature and radiation when incorporated in a three-dimensional macromolecule. The structural similarity among the aromatic fractions of the insoluble matter of carbonaceous meteorites indicates that these aromatics were incorporated at an early stage and remained stable [59]. Aromatic material in the gas phase and in macromolecular form makes up a substantial fraction of the carbon in the interstellar medium, in comets, as well as in comets and meteorites. It is conceivable that these molecules played an important role in the emergence of life [59].

Figure 14 shows four mass spectra of PAHs recorded with our LIMS instrument in desorption mode [30]. The parent mass peak is observed in the mass spectra as the largest peak together with a few large-mass fragment peaks, which allows

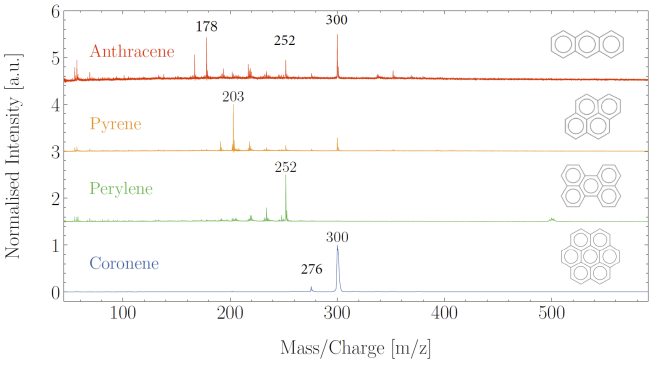

Figure 14: LIMS mass spectra recorded in desorption mode of four PAH species [30]. From bottom to top, the PAHs displayed are coronene (blue), perylene (green), pyrene (orange), and anthracene (red). A concentration of 100 µM has been used for all PAHs in this measurement. Prominent peaks are indicated in the plot. The spectra have been normalized to the highest peak for the respective PAH and have been offset from each other. The chemical structure of the PAHs is shown on the right side.

for good identification of these PAHs in a mixture of species, abiotic and biotic.

Another group of molecules closely related to life comprises the nucleobases. Nucleobases are the information-carrying components of the polynucleotidic polymers known as DNA and RNA, the molecules used by all terrestrial life forms to store their hereditary information. As such, DNA and RNA are essential to all known life forms, and, accordingly, intact polynucleotides have a very high diagnostic power; their detection and identification on an extraterrestrial body would be a very strong indicator of life [9]. The main issue with using DNA and RNA as a biosignature is their lack of robustness, i.e., both types of polymers would disintegrate in several thousand years, especially under harsh (radiation) conditions as found on, e.g., the surface of Mars [9, 10]. This molecular frailty makes DNA and RNA as intact polymer a low-priority biosignature, especially for extinct life. The nucleobases themselves are much more robust molecules, maintaining their molecular integrity on much longer timescales, and are much more readily detectable and identifiable by commonly used space compatible instruments. Despite these advantages, nucleobases alone are of limited value as biosignatures, mainly because all nucleobases also have

abiotic sources, and have even been shown to be produced in space. As a result, detecting nucleobases on an extraterrestrial body would be a relatively weak indicator of life. However, nucleobases could still play an important role in consolidating evidence for extinct or extant life, through simultaneous detection with multiple other biosignatures (e.g., lipids, amino acids, isotope fractionation). Accordingly, the possibility to detect nucleobases should still be considered valuable for any instrument aimed at detecting life beyond Earth. Therefore, measurements on nucleobases using our LIMS system operated in desorption mode are planned for the near future.

7. SUMMARY

The detection of signatures of life, past or present, on planetary objects other than the Earth, is of the highest interest in current space research and is of large interest for society in general. The biological signatures to be measured are of morphological and chemical nature, thus, appropriate instruments that can operate on the space platform are required to reliably identify these biosignatures. Several missions addressing the search for life are in the implementation phase, are in planning, are/or will be proposed in the near future. Moreover, biological experiments are foreseen within the activities of the Artemis mission of NASA [69].

For reliable detection of bio-signatures *in situ* on Solar System objects the detection of chemical and morphological signatures is necessary [10], and the combination of these will allow for a robust assessment if life has been detected or not. With the instrument developments over the past decade, we demonstrated that with our LIMS instrument we cover the following groups of bio-signatures (see Figure 1):

v) quantitative element abundance

ii) element distribution, in 2D and 3D, for microscopic features in the samples

iii) microscopic imaging for morphology

iv) biological signatures in isotope

v) complex organic molecules

Together with macroscopic imaging, this covers the full set of biosignatures for life detection, as defined for the search for life on Mars [13]. To add complementary measurements, high spatial resolution Raman spectroscopy, laser-induced breakdown spectroscopy (LIBS), or laser-induced native fluorescence (LINF) might be considered [11].

ACKNOWLEDGEMENTS

The financial support by the Swiss National Science Foundation (grant 200020_184657), the NCCR PlanetS (grant 51NF40-182901), and Swiss National Science Foundation Ambizione grant (grant PZ00P2_193453) are gratefully acknowledged.

REFERENCES

[1] N. Mangold, S. Gupta, O. Gasnault, G. Dromart, J. D. Tarnas, S. F. Sholes, B. Horgan, C. Quantin-Nataf, A. J. Brown, S. Le Mouélic, R. A. Yingst, J. F. Bell, O. Beyssac, T. Bosak1, F. Calef III, B. L. Ehlmann, K. A. Farley, J. P. Grotzinger, K. Hickman-Lewis, S. Holm Alwmark, L. C. Kah, J. Martinez-Frias, S. M. McLennan, S. Maurice, J. I. Nuñez, A. M. Ollila, P. Pilleri, J. W. Rice Jr., M. Rice, J. I. Simon, D. L. Shuster, K. M. Stack, V. Z. Sun, A. H. Treiman, B. P. Weiss, R. C. Wiens, A. J. Williams, N. R. Williams, K. H. Williford, Perseverance rover reveals an ancient delta-lake system and flood deposits at Jezero crater, Mars, Science (2021), in press, DOI: 10.1126/science.abl4051.

[2] K.P. Hand, A.E. Murray, J.B. Garvin, W.B. Brinckerhoff, B.C. Christiner, K.S. Edgett, B.L. Ehlmann, C.R. German, A.G. Hays, T.M. Hoehler, S.M. Hörst, J.I. Lunine, K.H. Nealson, C. Paranicas, B.E. Schmidt, D.E. Smith, A.R. Rhoden, M.J. Russel, A.S. Templeton, P.A. Willis, R.A. Yingst, C.B. Phillips, M.L. Cable, K.L. Craft, A.E. Hofmann, T.A. Nordheim, R.P. Pappalardo, and P.E. Team, (2017) Report of the European Lander Science Defintion Team.

[3] M.L. Cable, C. Porco, C.R. Glein, C.R. German, S.M. MacKenzie, M. Neveu, T.M. Hoehler, A.E. Hofmann, A.R. Hendrix, J. Eigenbrode, F. Postberg, L.J. Spilker, A. McEwen, J.H. Waite, P. Wurz, J. Helbert, A. Anbar, J.-P. de Vera, and J. Núñez, The Science Case for a Return to Enceladus, Planet. Sci. Jou., 2:132 (2021), 12 pages, DOI: 10.3847/PSJ/abfb7a.

[4] Noam R. Izenberg, Diana M. Gentry, David J. Smith, Martha S. Gilmore, David H. Grinspoon, Mark A. Bullock, Penelope J. Boston, and Grzegorz P. Słowik, The Venus Life Equation, Astrobiology, 21(8), (2021), DOI: 10.1089/ast.2020.2326

[5] P. Mahaffy, C.R. Webster, M. Cabane, P.G. Conrad, P. Coll, S. K. Atreya, R. Arvey, M. Barciniak, M. Benna, L. Bleacher, W. B. Brinckerhoff, J.L. Eigenbrode, D. Carignan, M. Cascia, R.A. Chalmers, J.P. Dworkin, T. Errigo, P. Everson, H. Franz, R. Farley, S. Feng, G. Frazier, C. Freissinet, D. P. Glavin, D. N. Harpold, D. Hawk, V. Holmes, C.S. Johnson, A. Jones, P. Jordan, J. Kellogg, J. Lewis, E. Lyness, C.A. Malespin, D.K. Martin, J. Maurer, A.C. McAdam, D. McLennan, T.J. Nolan, M. Noriega, A.A. Pavlov, B. Prats, E. Raaen, O. Sheinman, D. Sheppard, J. Smith, J.C. Stern, F. Tan, M. Trainer, D. W. Ming, R. V. Morris, J. Jones, C. Gundersen, A. Steele, J. Wray, O. Botta, L.A. Leshin, T. Owen, S. Battel, B. M. Jakosky, H. Manning, S. Squyres, R. Navarro-González, C. P. McKay, F. Raulin, R. Sternberg, A. Buch, P. Sorensen, R. Kline-Schoder, D. Coscia, C. Szopa, S. Teinturier, C. Baffes, J. Feldman, G. Flesch, S. Forouhar, R. Garcia, D. Keymeulen, S. Woodward, B. P. Block, K. Arnett, R. Miller, C. Edmonson, S. Gorevan, E. Mumm, The Sample

Analysis at Mars Investigation and Instrument Suite, Sp. Sci. Rev., 170, (2012) 401–478

[6] J.L. Eigenbrode, R.E. Summons, A. Steele, C. Freissinet, M. Millan, R. Navarro-González, B. Sutter, A.C. McAdam, H.B. Franz, D.P. Glavin, P.D. Archer, P.R. Mahaffy, P.G. Conrad, J.A. Hurowitz, J.P. Grotzinger, S. Gupta, D.W. Ming, D.Y. Sumner, C. Szopa, C. Malespin, A. Buch, and P. Coll, Organic matter preserved in 3-billion-year-old mudstones at Gale crater, Mars, Science 360 (2018) 1096–1101, DOI: 10.1126/science.aas9185.

[7] F. Goesmann, W.B. Brinckerhoff, F. Raulin, W. Goetz, R.M. Danell, S.A. Getty, S. Siljeström, H. Mißbach, H. Steininger, R.D. Arevalo Jr., A. Buch, C. Freissinet, A. Grubisic, U.J. Meierhenrich, V.T. Pinnick, F. Stalport, C. Szopa, J.L. Vago, R. Lindner, M.D. Schulte, J.R. Brucato, D.P. Glavin, N. Grand, X. Li, and F.H. W. van Amerom; the MOMA Science Team, The Mars Organic Molecule Analyzer (MOMA) Instrument: Characterization of Organic Material in Martian Sediments, Astrobiology 17(6/7), (2017) 655–685, DOI: 10.1089/ast.2016.1551.

[8] W. Goetz, W.B. Brinckerhoff, R. Arevalo Jr., C. Freissinet, S. Getty, D.P. Glavin, S. Siljeström, A. Buch, F. Stalport, A. Grubisic, X. Li, V. Pinnick, R. Danell, F.H.W. van Amerom, F. Goesmann, H. Steininger, N. Grand, F. Raulin, C. Szopa, U. Meierhenrich, J.R. Brucato and the MOMA Science Team, MOMA: the challenge to search for organics and biosignatures on Mars, International Journal of Astrobiology 15(3), (2016), 239-250, doi: 10.1017/S1473550416000227.

[9] Zita Martins, In situ biomarkers and the Life Marker Chip, Astronomy & Geophysics, Volume 52 (1), (2011), 1.34–1.35, DOI: 10.1111/j.1468-4004.2011.52134.x

[10] J.W. Aerts, W.F.M. Röling, A. Elsaesser, and P. Ehrenfreund, Biota and Biomolecules in Extreme Environments on Earth: Implications for Life Detection on Mars, Life, 4, (2014) 535-565, DOI: 10.3390/life4040535

[11] A. Stevens, A. McDonald, C. de Koning, A. Riedo, L. Preston, P. Ehrenfreund, P. Wurz, and C. Cockell, Detectability of biosignatures in a low-biomass simulation of martian sediments, Nature Sci. Rep., 9:9706 (2019), 12 pages, DOI: 10.1038/s41598-019-46239-z.

[12] A. Riedo, C. de Koning, A.H. Stevens, C.S. Cockell, A. McDonald, A. Cedeño López, V. Grimaudo, M. Tulej, P. Wurz, and P. Ehrenfreund, The detection of elemental signatures of microbes in Martian mudstone analogues using high-spatial resolution laser ablation ionization mass spectrometry, Astrobiology 20(10), (2020), 12 pages, DOI: 10.1089/ast.2019.2087.

[13] J.F. Mustard, M. Adler, A. Allwood, D.S. Bass, D.W. Beaty, J.F. Bell III, W.B. Brinckerhoff, M. Carr, D.J. Des Marais, B. Drake, K.S. Edgett, J. Eigenbrode, L.T. Elkins-Tanton, J.A. Grant, S. M. Milkovich, D. Ming, C. Moore, S. Murchie, T.C. Onstott, S.W. Ruff, M.A. Sephton, A. Steele, A. Treiman (2013): Report of the Mars 2020 Science Definition Team, 154 pp., posted July, 2013, by the Mars Exploration Program Analysis Group (MEPAG) at http://mepag.jpl.nasa.gov/reports/MEP/Mars_2020_SDT_Report_Final.pdf.

[14] P. Wurz, M. Tulej, A. Riedo, V. Grimaudo, R. Lukmanov, and N. Thomas, Investigation of the Surface Composition by Laser Ablation/Ionisation Mass Spectrometry, IEEE Aerospace Conference Big Sky, MT, USA, (2021), 50100, 15 pages, DOI: 10.1109/AERO50100.2021.9438486.

[15] V. Grimaudo, P. Moreno-García, A. Riedo, M.B. Neuland, M. Tulej, P. Broekmann, and P. Wurz, High-Resolution Chemical Depth Profiling of Solid Material Using a Miniature Laser Ablation/Ionization Mass Spectrometer, Analytical Chemistry, 87 (2015) 2037–2041, DOI: 10.1021/ac504403j.

[16] V. Grimaudo, P. Moreno-García, A. Riedo, S. Meyer, M. Tulej, M.B. Neuland, M. Mohos, C. Gütz, S.R. Waldvogel, P. Wurz, and P. Broekmann, Toward Three-Dimensional Chemical Imaging of Ternary Cu–Sn–Pb Alloys Using Femtosecond Laser Ablation/Ionization Mass Spectrometry, Analytical Chemistry, 89, (2017) 1632–1641, DOI: 10.1021/acs.analchem.6b03738.

[17] A. Neubeck, M. Tulej, M. Ivarsson, C. Broman, A. Riedo, S. McMahon, P. Wurz, and S. Bengtson, Mineralogical determination in situ of a highly heterogeneous material using a miniaturized laser ablation mass spectrometer with high spatial resolution, International Journal of Astrobiology, 15, (2015) 133–146, DOI: 10.1017/S1473550415000269.

[18] A. Riedo, A. Bieler, M. Neuland, M. Tulej, and P. Wurz, Performance evaluation of a miniature laser ablation time-of-flight mass spectrometer designed for in situ investigations in planetary space research, Journal of Mass Spectrometry, 48 (2013) 1–15, DOI: 10.1002/jms.3157.

[19] A. Riedo, C. de Koning, A. Stevens, A. McDonald, A.C. López, M. Tulej, P. Wurz, C.S. Cockell, and P. Ehrenfreund, The detection of microbial life fingerprint in Martian mudstone analogues using high spatially resolved laser ablation ionization mass spectrometry. Astrobiology, 20(10), (2020), 12 pages, DOI: 10.1089/ast.2019.2087.

[20] A. Riedo, M. Neuland, S. Meyer, M. Tulej, and P. Wurz, Coupling of LMS with a fs-laser ablation ion source: elemental and isotope composition measurements, Journal of Analytical Atomic Spectrometry, 28, (2013), 1256–1269, DOI: 10.1039/C3JA50117E.

[21] M. Tulej, N.F.W. Ligterink, C. de Koning, V. Grimaudo, R. Lukmanov, P. Keresztes Schmidt, A. Riedo, and P. Wurz, Current Progress in Femtosecond Laser Ablation/ Ionisation Time-of-Flight Mass Spectrometry, Applied Sciences, 11, (2021), 2562, DOI: 10.3390/app11062562.

[22] M. Tulej, A. Neubeck, M. Ivarsson, A. Riedo, M.B. Neuland, S. Meyer, and P. Wurz, Chemical Composition of Micrometer-Sized Filaments in an Aragonite Host by a Miniature Laser Ablation/Ionization Mass Spectrometer, Astrobiology, 15, (2015) 669–682., DOI: 10.1089/ast.2015.1304.

[23] S. Meyer, A. Riedo, M.B. Neuland, M. Tulej, and P. Wurz, Fully automatic and precise data analysis developed for time-of-flight mass spectrometry, Journal of Mass Spectrometry, 52, (2017), 580–590, DOI: 10.1002/jms.3964.

[24] R. Wiesendanger, D. Wacey, M. Tulej, A. Neubeck, M. Ivarsson, V. Grimaudo, P. Moreno, A. Cedeño López, A. Riedo, and P. Wurz, Chemical and optical identification of micrometer-sized 1.9 billion-year-old fossils by combining a miniature laser ablation ionization mass spectrometry system with an optical microscope, Astrobiology, 18, (2018), 1071–1080, DOI: 10.1089/ast.2017.1780.

[25] Roland Hergenröder, Laser-generated aerosols in laser ablation for inductively coupled plasma spectrometry, Spectrochimica Acta Part B 61 (2006) 284–300, DOI: 10.1016/j.sab.2006.02.001

[26] A. Riedo, Lukmanov R., Grimaudo V., de Koning C., Ligterink N. F. W., Tulej M., and Wurz P. (2021) Improved plasma stoichiometry recorded by LIMS by using a double-pulse femtosecond laser ablation ion source. Rapid Communications in Mass Spectrometry, 35:e9094 (2021), 8 pages, DOI: 10.1002/rcm.9094.

[27] M. Tulej, R. Wiesendanger, A. Riedo, G. Knopp, and P. Wurz, Mass spectrometric analysis of the Mg plasma produced by double-pulse femtosecond laser irradiation, Journal of Analytical Atomic Spectrometry, 33, (2018) 1292–1303, DOI: 10.1039/C8JA00036K.

[28] P. Wurz, K.R. Lykke, M.J. Pellin, D.M. Gruen, D.H. Parker, Characterization of Fullerenes by Laser-Based Mass Spectrometry, Vacuum 43 (1992), 381–385.

[29] N.F.W. Ligterink, V. Grimaudo, P. Moreno-García, R. Lukmanov, M. Tulej, I. Leya, R. Lindner, P. Wurz, C.S. Cockell, P. Ehrenfreund, and A. Riedo, ORIGIN: a novel and compact Laser Desorption — Mass Spectrometry system for sensitive in situ detection of amino acids on extraterrestrial surfaces, Nature Science Reports 10:9641, (2020), 10 pages, DOI: 10.1038/s41598-020-66240-1.

[30] K. Kipfer, N.F.W. Ligterink, J. Bouwman, L. Schwander, V. Grimaudo, C. de Koning, N. Boeren, P. Keresztes Schmidt, R. Lukmanov, M. Tulej, P. Wurz, and A. Riedo, Towards Detecting Carbon Chemistry on Planetary Objects with the ORIGIN Space Instrument, Planet. Sci. Jou. (2021), submitted.

[31] S. Frey, R.Wiesendanger, M. Tulej, M. Neuland, A. Riedo, V. Grimaudo, P. Moreno-García, A. Cedeño López, M. Mohos, B. Hofmann, K. Metzger, P. Broekmann, and P. Wurz, Chemical analysis of a lunar meteorite by laser ablation mass spectrometry, Planet. Sp. Science (2020), 182, 104816, DOI: 10.1016/j.pss.2019.104816.

[32] M. Neuland, K. Mezger, A. Riedo, M. Tulej, and P. Wurz, The chemical composition and homogeneity of the Allende matrix, Planet. Sp. Sci. 204 (2021) 105251, DOI: 10.1016/j.pss.2021.105251.

[33] M. Tulej, R. Lukmanov, V. Grimaudo, A. Riedo, C. de Koning, N.F.W. Ligterink, A. Neubeck, M. Ivarson, and P. Wurz, Determination of the microscopic mineralogy of inclusion in an amygdaloidal pillow basalt by fs-LIMS, Jou. Anal. At. Spect. 36(1), (2020), 80–91, DOI: 10.1039/D0JA00390E.

[34] U. von Stockar and J.-S. Liu, Does microbial life always feed on negative entropy? Thermodynamic analysis of microbial growth, Biochimica et Biophysica Acta, 1412 (1999) 191–211, DOI: 10.1016/S0005-2728(99)00065-1.

[35] Victor Parro, Graciela de Diego-Castilla, Mercedes Moreno-Paz, Yolanda Blanco, Patricia Cruz-Gil, José A. Rodríguez-Manfredi, David Fernández-Remolar, Felipe Gómez, Manuel J. Gómez, Luis A. Rivas, Cecilia Demergasso, Alex Echeverría, Viviana N. Urtuvia, Marta Ruiz-Bermejo, Miriam García-Villadangos, Marina Postigo, Mónica Sánchez-Román, Guillermo Chong-Diaz, and Javier Gómez-Elvira, A Microbial Oasis in the Hypersaline Atacama Subsurface Discovered by a Life Detector Chip: Implications for the Search for Life on Mars, Astrobiology 11(10), (2011), 969–996, DOI: 10.1089/ast.2011.0654

[36] Víctor Parro, Graciela de Diego-Castilla, José A. Rodríguez-Manfredi, Luis A. Rivas, Yolanda Blanco-López, Eduardo Sebastián, Julio Romeral, Carlos Compostizo, Pedro L. Herrero, Adolfo García-Marín, Mercedes Moreno-Paz, Miriam García-Villadangos, Patricia Cruz-Gil, Verónica Peinado, Javier Martín-Soler, Juan Pérez-Mercader, and Javier Gómez-Elvira, SOLID3: A Multiplex Antibody Microarray-Based Optical Sensor Instrument for In Situ Life Detection in Planetary Exploration, Astrobiology, 11(1), (2011), 15–28, DOI: 10.1089/ast.2010.0501

[37] A. Cedeño López, V. Grimaudo, A. Riedo, M. Tulej, R. Wiesendanger, R. Lukmanov, P. Moreno-García, E. Lörtscher, P. Wurz, and P. Broekmann, Three-Dimensional Compositional Analysis of SnAg Solder Bumps

using Ultraviolet Femtosecond Laser Ablation Ionization Mass Spectrometry, Anal. Chem. 92 (2020a), 1355-1362, DOI: 10.1021/acs.analchem.9b04530.

[38] V. Grimaudo, P. Moreno-García, A. Riedo, S. Meyer, M. Tulej, M.B. Neuland, C. Gütz, S. Waldvogel, P. Wurz, and P. Broekmann, 3D chemical imaging of ternary Cu-Sn-Pb alloys using Femtosecond Laser Ablation/Ionization Mass Spectrometry, Anal. Chem. 89(3), (2017) 1632–1641, DOI: 10.1021/acsanalchem.6b03738

[39] R.A. Lukmanov, M. Tulej, N.F.W. Ligterink, C. De Koning, A. Riedo, V. Grimaudo, A. Neubeck, D. Wacey, and P. Wurz, Chemical identification of microfossils from the 1.88 Ga Gunflint chert. Towards empirical biosignatures using LIMS, Journal of Chemometrics 2021;e3370 (2021), 16 pages, DOI: 10.1002/cem.3370.

[40] R.A. Lukmanov, A. Riedo, D. Wacey, N.F.W. Ligterink, V. Grimaudo, M. Tulej, C. De Koning, A. Neubeck, and P. Wurz, On Topological analysis of fs-LIMS data. Implications for in situ planetary mass spectrometry, Frontiers in Artificial Intelligence 4:668163 (2021), 12 pages, DOI: 10.3389/frai.2021.668163.

[41] R.A. Lukmanov, Characterization of bio-organic and inorganic chemistries using Laser-based Mass Spectrometry, PhD thesis, (2021), University of Bern, Switzerland.

[42] L. McInnes, Healy J., and J. Melville, UMAP: Uniform manifold approximation and projection for dimension reduction, arXiv preprint, (2018) arXiv:1802.03426.

[43] G. Singh, F. Mémoli, and G.E. Carlsson, Topological methods for the analysis of high dimensional data sets and 3D object recognition, in *Eurographics Symposium on Point-Based Graphics*, 91, (2007), 91–100, DOI: 10.2312/SPBG/SPBG07/091-100.

[44] M. Tulej, A. Riedo, M.B. Neuland, S. Meyer, D. Lasi, D. Piazza, N. Thomas, and P. Wurz, A miniature instrument suite for in situ investigation of the composition and morphology of extraterrestrial materials, Geostand. Geoanal. Res., 38 (2014), 441–466, DOI: 10.1111/j.1751-908X.2014.00302.x.

[45] A. Riedo, S. Meyer, B. Heredia, M.B. Neuland, A. Bieler, M. Tulej I. Leya, M. Iakovleva, K. Mezger and P. Wurz, Highly accurate isotope composition measurements by a miniature laser ablation mass spectrometer designed for in situ investigations on planetary surfaces, Planet. Space Sci. 87 (2013), 1–13, DOI: 10.1016/j.pss.2013.09.007.

[46] A. Riedo, V. Grimaudo, J. Aerts, R. Lukmanov, M. Tulej, P. Broekmann, R. Lindner, P. Wurz and P. Ehrenfreund, Laser Ablation Ionization Mass Spectrometry: A space prototype system for in situ Sulphur isotope fractionation analysis on planetary surfaces, Frontiers in Astronomy and Space Sciences Astrobiology, 8:726373 (2021), 8 pages, DOI: 10.3389/fspas.2021.726373.

[47] R. Amils, E. González-Toril, D. Fernández-Remolar, F. Gómez, Á. Aguilera, N. Rodríguez, M. Malki, A. García-Moyano, A.G. Fairén, V. de la Fuente, and J. Luis Sanz, Extreme environments as Mars terrestrial analogs: The Rio Tinto case, Planetary and Space Science, 55, (2007) 370–381, DOI: 10.1016/j.pss.2006.02.006.

[48] Y. Chen, L. Wu, R. Boden, A. Hillebrand, D. Kumaresan, H. Moussard, M. Baciu, Y. Lu, and J. Colin Murrell, Life without light: microbial diversity and evidence of sulfur- and ammonium-based chemolithotrophy in Movile Cave, The ISME Journal, 3 (2009) 1093–1104, DOI: 10.1038/ismej.2009.57.

[49] D. Kumaresan, J. Stephenson, A.C. Doxey, H. Bandukwala, E. Brooks, A. Hillebrand-Voiculescu, A.S. Whiteley, and J.C. Murrell, Aerobic proteobacterial methylotrophs in Movile Cave: genomic and metagenomic analyses, Microbiome, 6(1), (2018), DOI: 10.1186/s40168-017-0383-2.

[50] D. Kumaresan, D. Wischer, J. Stephenson, A. Hillebrand-Voiculescu, and J.C. Murrell, Microbiology of Movile Cave—A Chemolithoautotrophic Ecosystem, Geomicrobiology Journal, 31, (2014), 186–193, DOI: 10.1080/01490451.2013.839764.

[51] S.M. Sarbu, C. Lascu, and T. Brad, Dobrogea: Movile Cave, in *Cave and Karst Systems of Romania*, edited by G.M.L. Ponta and B.P. Onacs, Springer International Publishing, Cham, (2019) pp 429–436.

[52] G. Ratié, D. Jouvin, J. Garnier, O. Rouxel, S. Miska, E. Guimarães, L. Cruz Vieira, Y. Sivry, I. Zelano, E. Montarges-Pelletier, F. Thil, and C. Quantin, Nickel isotope fractionation during tropical weathering of ultramafic rocks, Chem. Geol. 402 (2015), 68–76, DOI: 10.1016/j.chemgeo.2015.02.039.

[53] W. Bach, M. Rosner, N. Jöns, Svenja Rausch, Laura F. Robinson, Holger Paulick, and Jörg Erzinger, Carbonate veins trace seawater circulation during exhumation and uplift of mantle rock: results from ODP Leg 209. Earth Planet Sci. Lett., 311(3–4), (2011), 242–252.

[54] M. Tulej, A. Neubeck, A. Riedo, R. Lukmanov, V. Grimaudo, N.F.W. Ligterink, M. Ivarson, W. Bach, C. de Koning, and P. Wurz, Isotope abundance ratio measurements using femtosecond laser ablation ionization mass spectrometry, Jou. Mass Spectrom. 55(e4660), (2020), 16 pages, DOI: 10.1002/jms.4660.

[55] M. Tulej, A. Neubeck, M. Ivarsson, A. Riedo, M.B. Neuland, S. Meyer, and P. Wurz, Chemical composition of micrometre-sized filaments in an aragonite host by a miniature laser ablation/□onization mass spectrometer, Astrobiology 15(8), (2015) 669–682, doi: 10.1089/ast.2015.1304.

[56] C. D. Georgiou and D. W. Deamer, Lipids as Universal Biomarkers of Extraterrestrial Life, Astrobiology, 14, (2014), 541–549, DOI: 10.1089/ast.2013.1134

[57] A. F. Davila and C. P. McKay, Chance and Necessity in Biochemistry: Implications for the Search for Extraterrestrial Biomarkers in Earth-like Environments, Astrobiology, 14, (2014), 534–540, DOI: 10.1089/ast.2014.1150.

[58] M.A. Sephton, J.H. Waite, and T.G. Brockwell, How to Detect Life on Icy Moons, Astrobiology, 18(7), (2018), 834-855, DOI: 10.1089/ast.2017.1656

[59] P. Ehrenfreund, S. Rasmussen, J. Cleaves, and L. Chen, Experimentally Tracing the Key Steps in the Origin of Life: The Aromatic World, Astrobiology, 6(3), 490-520, DOI: 10.1089/ast.2006.6.490

[60] K. Kvenvolden, J. Lawless, K. Pering, E. Peterson, J. Flores, C. Ponnamperuma, I.R. Kaplan, C. Moore, Evidence for Extraterrestrial Amino-acids and Hydrocarbons in the Murchison Meteorite, Nature 228 (1970) 923–926, DOI: 10.1038/228923a0.

[61] M. H. Engel, S. A. Mackot, and J. A. Silfer, Carbon isotope composition of individual amino acids in the Murchison meteorite, Nature 348 (1990), 47–49, DOI: 10.1038/348047a0

[62] Y. Lu, and S. Freeland, On the evolution of the standard amino-acid alphabet, Genome Biology 7 (2006), doi:10.1186/gb-2006-7-1-102.

[63] P. Ehrenfreund, and S. B. Charnley, Organic molecules in the interstellar medium, comets, and meteorites: A voyage from dark clouds to the early Earth, Annual Review of Astronomy and Astrophysics 38, (2000) 427–483, DOI: 10.1146/annurev.astro.38.1.427.

[64] I. Wagner, H. Musso, New Naturally Occurring Amino Acids, Angewandte Chemie, 22 (1983), 816–828, DOI: 10.1002/anie.198308161.

[65] K. P. Hand, A.E. Murray, J.B. Garvin, W.B. Brinckerhoff, B.C. Christner, K.S. Edgett, B.L. Ehlmann, C.R. German, A.G. Hayes, T.M. Hoehler, S.M. Hoerst, J.L. Lunine, K.H. Nealson, C. Paranicas, B.E. Schmidt, D.E. Smith, A.R. Rhoden, M.J. Russell, A.S. Templeton, P.A. Willis, R.A. Yingst, C.B. Phillips, M.L. Cable, K. L. Craft., A. E. Hofmann, T. A. Nordheim, R.P. Pappalardo, and the Project Engineering Team, Report of the European Lander Science Definition Team, (2017).

[66] P. G. Higgs and R. E. Pudritz. A thermodynamic basis for prebiotic amino acid synthesis and the nature of the first genetic code, Astrobiology 9(5), (2009) 483–490.

[67] M. B. Wilhelm, A. J. Ricco, M. Chin, J. L. Eigenbrode, L. Jahnke, P. M. Furlong, D. K. Buckner, T. Chinn, K. Sridhar, T. McClure, T. Boone, L. Radosevich, A. Rademacher, T. Hoac, M. Anderson, S. Getty, A. Southard, R. Williams, X. Li, T. Smith, O. Podlaha, and J. van Winden, ExCALiBR: An Instrument for Uncovering the Origin of the Moon's Organics, Lunar Surface Science Workshop, (2020), Abstract id 2241

[68] N. Boeren, V. Grimaudo, S. Gruchola, C. de Koning, P. Keresztes Schmidt, K. Kipfer, N.F.W. Ligterink, R. Lukmanov, M. Tulej, P. Wurz, and A. Riedo, Detecting lipids on planetary surfaces with laser-based mass spectrometry, Planet. Sci. Jou. (2021), submitted.

[69] Artemis III, Science Definition Report, NASA/SP-20205009602

BIOGRAPHY

Peter Wurz *has a degree in electronic engineering (1985), an M.Sc. and a Ph.D. in Physics from Technical University of Vienna, Austria (1990). He has been a post-doctoral researcher at Argonne National Laboratory, USA. Since 1992 at the University of Bern. He is Professor of physics and since 2015 head of the Space Science and Planetology division. He has been Co-I and PI for many science instruments for space missions of ESA, NASA, ISRO, CNSA, Roscosmos, and JAXA.*

Marek Tulej *received a Ph.D. in Physical Chemistry from the University of Basel, Switzerland in 1999. After his post-doctoral period at Paul Scherrer Institute (PSI), Switzerland, he joined in 2008 the University of Bern as an instrument scientist for space missions, including Phobos-Grunt, Marco Polo-R, Luna-Resurs, and JUICE.*

Valentine Grimaudo *received a Ph.D in Chemistry and Molecular Sciences from the University of Bern, Switzerland, in 2018, where she developed new measurement procedures based on LIMS for the chemical analysis of industrial process in the interconnect technology. After her degree she joined the Space Science and Planetology division at the University of Bern as post-doctoral researcher.*

Rustam Lukmanov *did a BSc and a MSc in Geology, St.-Petersburg State University, Russia, where he worked on Microanalytical studies of the iron oxidation state in mantle spinels. Since 2017 he is at the University of Bern, and in 2021 he finished his PhD on the investigation fossils in minerals to characterize early life with the LIMS instrument.*

Salome Gruchola *received her B.Sc. and M.Sc. in experimental physics from the University of Bern, Switzerland. She continued her studies at the University of Bern as a Ph.D student where she is currently working on the investigation of early life by studying microfossils with LIMS.*

Kristina Kipfer *received her B.Sc. and M.Sc. in experimental Physics with special qualification in Astronomy at the university of Bern, Switzerland. She is currently working as a PhD student in Bern where she is studying the properties of interstellar and planetary ices with LIMS instruments.*

Coenraad de Koning *has a B. Sc. in Chemistry and a M. Sc. in Biomolecular Sciences, with a special qualification in Chemical Biology, from the Vrije Universteit Amsterdam, the Netherlands. He is currently a Ph.D. student at the University of Bern, Switzerland, where he is currently working towards improved performance in element and isotope analysis using a new high resolution LIMS instrument.*

Nikita Boeren *received her B.Sc. in BioAnalytical Chemistry and M.Sc. in Molecular Sciences, both at the VU University Amsterdam, The Netherlands. She is currently working as a PhD student in Bern, Switzerland, where she is studying the detection of bio-relevant molecules with the LIMS instrument.*

Loraine Schwander *received her B.Sc. in Biology with specialization in Cell Biology in 2019 and her M.Sc. in Bioinformatics and Computational Biology in 2021, both from the University of Bern. She undertook an interdisciplinary Master's thesis at the Space Science and Planetology Division at the University of Bern where she did a performance analysis of a novel LDMS instrument with special focus on the detection of amino acids in two permafrost samples.*

Peter Keresztes Schmidt *received his B.Sc. and M.Sc. in Chemistry at the ETH Zürich, Switzerland. He is currently working as a PhD student in Bern, Switzerland, where he is developing a new the LIMS instrument for in situ studies on the lunar surface.*

Niels F.W. Ligterink *received his Ph.D. in astrophysics from the Leiden Observatory, Leiden University, The Netherlands, after completing a B.Sc. in chemistry and M.Sc. in physical chemistry at the Free University, Amsterdam, The Netherlands. Since 2018 he is based in Bern, first as a Center for Space and Habitability experimental post-doc and currently as a SNSF Ambizione fellow, where he uses LIMS space instruments to investigate physicochemical properties of interstellar and planetary ices.*

Andreas Riedo *received his Ph.D. in Physics in 2014 from the University of Bern, Switzerland. In 2016 he received a SNSF fellowship that allowed him to continue his research in Astrobiology at the Leiden University, The Netherlands. He extended his stay at the Leiden University with a MCSA fellowship for another two years before he moved in 2019 to the Free University Berlin after receiving the prestigious Einstein fellowship. In 2020 he moved to University of Bern and is currently appointed as researcher and project manager within ESA's JUICE space mission.*